LES of the turbulent compressible flow spatially developing in a plane channel.

CHRISTOPHE BRUN[a], **MARGARETA PETROVAN BOIARCIUC**[b], **MICHAEL MANHART**[c]

a. Laboratoire des Ecoulements Géophysiques et Industriels, Université J. Fourier, 38000 Grenoble, France
b. Polytech'Orléans, Institut Prisme, 45000 Orléans, France
c. Technische Universität München, Fachgebiet Hydromechanik, Arcisstrasse 21, 80333 Munich, Germany

Résumé :

On présente des Simulations des Grandes Echelles de l'écoulement turbulent qui se développe dans un canal plan de longueur $88\ h$ *à* $Re = 4880$ *0.7* $M = 0.7$. *L'effet de conditions d'entrées réalistes de conditions de sorties faiblement réfléchissantes sera analysé et discuté. Des cas d'écoulement supersonique avec distorsion par effet de gradient de pression adverse seront considérés par la suite.*

Abstract :

Large Eddy Simulation of the turbulent flow which spatially develops in a plane channel with a length of $88\ h$ *will be presented for* $Re = 4880$ *and* $M = 0.7$. *The effect of realistic inflow conditions and low reflective outflow conditions will be analysed and discussed. Supersonic channel flow case and distorsion of the flow by mean of adverse pressure gradient will be further considered.*

Mots clefs : LES ; compressible channel flow, numerical soft boundary conditions

There exist in the literature many numerical simulations of compressible turbulent flow developed in a channel by mean of driven source terms to model pressure drop effects [1, 2, 3, 4, 5, 6, 7, 8]. Concerning the direct simulation of the compressible flow developing in a channel there is no publications in the literature, but the low Reynolds number study performed by Poinsot and Lele [9] to assess a set of soft inlet and outlet boundary conditions for compressible flows. The purpose of the present study is to adress partly this issue based on the computation and the analysis of the 3D turbulent compressible flow developing in a plane channel using Large Eddy Simulation technique.

1 Governing equations

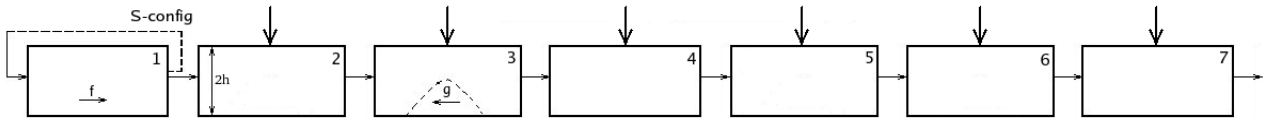

FIG. 1 – Geometry of the spatially developing channel flow

The flow geometry consists of a plane channel with a width $2\,h$ (figure 1). The fluid is assumed to be an ideal gas (air) with constant ratio of specific heats $\gamma = \frac{c_p}{c_v} = 1.4$, $R = c_p - c_v = 287 JKg^{-1}K^{-1}$ and constant Prandtl number $Pr = 0.7$. Isothermal-wall boundary conditions are imposed. The numerical code initialy developed in Grenoble LEGI and further in Poitiers LEA solves the Navier-Stokes (NS) equations presently written in a conservative form with Large Eddy Simulation technique. The NS equations are non-dimensionalized by the wall temperature T_w, the channel half-width h, the bulk-averaged density $\rho_b = \frac{1}{2h}\int_{-h}^{+h} \rho dy$, and the bulk mass flux $(\rho u)_b = \frac{1}{2h}\int_{-h}^{+h} \rho u dy$. The governing equations read in a conservative form

$$\frac{\partial \overline{\mathcal{U}}}{\partial t} + \frac{\partial \overline{\mathcal{F}_i}}{\partial x_i} = \mathcal{S}, \tag{1}$$

where $\overline{\mathcal{U}}$ is the vector of conservative variables, $\overline{\mathcal{U}} = (\overline{\rho},\ \overline{\rho u},\ \overline{\rho v},\ \overline{\rho w},\ \overline{\rho e})^t$, and $\overline{\mathcal{F}_i}$ is the the vector of filtered dimensionless fluxes respectively

$$\overline{(\mathcal{F}_i)}_1 = \bar{\rho}\tilde{u}_i \tag{2}$$

$$\overline{(\mathcal{F}_i)}_2 = \bar{\rho}\tilde{u}_i\tilde{u}_1 + \frac{1}{\gamma M^2}\varpi\delta_{i1} - \left(\frac{\tilde{\mu}}{Re} + \bar{\rho}\nu_{sgs}\right)\tilde{S}_{i1} \tag{3}$$

$$\overline{(\mathcal{F}_i)}_3 = \bar{\rho}\tilde{u}_i\tilde{u}_2 + \frac{1}{\gamma M^2}\varpi\delta_{i2} - \left(\frac{\tilde{\mu}}{Re} + \bar{\rho}\nu_{sgs}\right)\tilde{S}_{i2} \tag{4}$$

$$\overline{(\mathcal{F}_i)}_4 = \bar{\rho}\tilde{u}_i\tilde{u}_3 + \frac{1}{\gamma M^2}\varpi\delta_{i3} - \left(\frac{\tilde{\mu}}{Re} + \bar{\rho}\nu_{sgs}\right)\tilde{S}_{i3} \tag{5}$$

$$\overline{(\mathcal{F}_i)}_5 = \tilde{u}_i(\bar{\rho}\tilde{e} + \varpi) - \gamma M^2\frac{\tilde{\mu}}{Re}\tilde{u}_j\tilde{S_{ij}} - \frac{\gamma}{\gamma-1}\left(\frac{\tilde{\mu}}{RePr} + \frac{\bar{\rho}\nu_{sgs}}{Pr_{sgs}}\right)\frac{\partial\vartheta}{\partial x_i} \tag{6}$$

The equation of state (ideal gas law) closes the system of equations describing compressible fluid flow, based on the *macropressure* ϖ and the *macrotemperature* ϑ introduced by Comte & Lesieur [10],

$$\varpi \simeq \bar{\rho}\vartheta \tag{7}$$

The total energy (for a perfect gas) is defined as $\bar{\rho}\tilde{e} = \frac{\varpi}{\gamma-1} + \frac{\gamma M^2}{2}\bar{\rho}\tilde{u}_i^2$, and the traceless strain rate tensor is $\tilde{S}_{ij} = \frac{\partial\tilde{u}_i}{\partial x_j} + \frac{\partial\tilde{u}_j}{\partial x_i} - \frac{2}{3}\frac{\partial\tilde{u}_k}{\partial x_k}\delta_{ij}$. $\mathcal{S} = (0, f, 0, 0, \gamma M^2 W)^t$ consists of the source terms for the momentum and energy equations, which will be further defined for the description of inflow conditions.
Non-dimensional parameters are the Mach number $M = \frac{(\bar{\rho}\tilde{u})_b/\bar{\rho}_b}{\sqrt{\gamma R T_w}} = 0.7$, the Reynolds number $Re = \frac{(\bar{\rho}\tilde{u})_b h}{\mu(T_w)} 4,880$, and the Prandtl number $Pr = \frac{\nu}{k} = \frac{c_p\mu(\tilde{T})}{\lambda(\tilde{T})} = 0.7$. A power law $\mu = \mu(\tilde{T}) = \mu_w(\tilde{T}/T_w)^{0.7}$ is applied for the molecular dynamic viscosity, as a relatively good approximation of the Sutherland law.
Large-Eddy Simulations are performed with an eddy-viscosity and an eddy-diffusivity Sub-Grid Scale (SGS) model based on the Filtered Structure Function (FSF) [11, 12, 13]. Eddy-viscosity is given by $\nu_{sgs}^{FSF} = 0.0014\, C_K^{-3/2}\,\Delta\langle||\nabla^6\tilde{u}(x+r) - \nabla^6\tilde{u}(x)||^2\rangle_{||r||=\Delta}^{1/2}$. Eddy diffusivity is obtained from $\lambda_{sgs} = \frac{\mu_{sgs}c_p}{Pr_{sgs}}$ where the SGS Prandtl number is set constant $Pr_{sgs} = 0.6$. $C_K = 1.4$ is the Kolmogorov constant. This model has shown to be efficient for solving compressible boundary layers without inhibiting transition the turbulence.
The discretisation of the fluxes ($\mathcal{F}_1$, $\mathcal{F}_2$, $\mathcal{F}_3$) in each direction is performed based on an extension of a fully explicit Mc Cormack scheme, modified by Gottlieb & Turkel [14] to get second order in time and fourth order in space. Time advancement is split in two steps, a predictor and a corrector step, which results in a globally centered fourth order scheme. This predictor-corrector scheme is valid only for the inner points, excepting the two last points in each direction. For these points, the derivatives are defined by Kennedy & Carpenter [15]. This stencil will be applied only for the free boundaries (inflow and outflow). Each subdomain 1 to 7 consists of a plane channel with a height $L_y = 2h$ (channel half width), a length $L_x = 4\pi h$, a width $L_z = 4/3\pi h$, and contains 673,920 grid points distributed along the streamwise direction ($n_x = 128$), the spanwise direction ($n_z = 81$), and the transverse direction ($n_y = 65$) including a refinement at the wall to reach the first grid point at $y^+ = 0.2$. The full domain consists of about 4.7 million points and is treated using MPI parallelisation on 7 processors on NEC-SX8 IDRIS.

2 Inflow and outflow conditions

The flow is evolving spatially from domain 2 to domain 7 (Fig 1). A fully developed channel flow using streamwise periodic boundary conditions is computed for domain 1 in order to ensure realistic inflow conditions for domain 2. This procedure is necessary to develop time dependent realistic turbulent structures. Non-reflecting outflow conditions based on wave decomposition [16, 9] are applied at the outlet of domain 7. Characteristic analysis described by Thompson in [17, 18] is applied for Euler equations, and generalized to the viscous-diffusive Navier-Stokes equations by Poinsot & Lele [9]. It consists in decomposing hyperbolic equations into wave modes of velocity to determine which wave is propagating into and out of the computational domain. The behavior of the outward propagating waves is defined entirely by the solution at and within the boundary, whereas the inward propagating waves are specified as boundary conditions.
The Navier-Stokes equations (1) are converted to an equivalent set of wave equations, which represent nonlinear waves propagating at characteristic velocities in the x-direction only, as (for the laminar form)

$$\frac{\partial\rho}{\partial t} + d_1 + \frac{\partial}{\partial y}(\rho v) + \frac{\partial}{\partial z}(\rho w) = 0 \tag{8}$$

$$\frac{\partial(\rho u)}{\partial t} + u d_1 + \rho d_3 + \frac{\partial}{\partial y}(\rho u v) + \frac{\partial}{\partial z}(\rho u w) = \frac{1}{Re}\frac{\partial(\mu S_{1j})}{\partial x_j} \tag{9}$$

$$\frac{\partial(\rho v)}{\partial t} + v d_1 + \rho d_4 + \frac{\partial}{\partial y}(\rho v v + \frac{1}{\gamma M^2} p) + \frac{\partial}{\partial z}(\rho v w) = \frac{1}{Re}\frac{\partial(\mu S_{2j})}{\partial x_j} \tag{10}$$

$$\frac{\partial(\rho w)}{\partial t} + w d_1 + \rho d_5 + \frac{\partial}{\partial y}(\rho w v) + \frac{\partial}{\partial z}(\rho w w + \frac{1}{\gamma M^2} p) = \frac{1}{Re}\frac{\partial(\mu S_{3j})}{\partial x_j} \tag{11}$$

$$\frac{\partial(\rho e)}{\partial t} + \gamma M^2 \left[\frac{1}{2}(u_k u_k) d_1 + \rho u d_3 + \rho v d_4 + \rho w d_5\right] + \frac{d_2}{\gamma - 1} + \frac{\partial}{\partial y}\left[(\rho e + p) v\right] + \frac{\partial}{\partial z}\left[(\rho e + p) w\right] = \frac{\partial}{\partial x_j}\left(\gamma M^2 \frac{\mu}{Re} u_i S_{ij} + \frac{\gamma}{\gamma - 1}\frac{\mu}{RePr}\frac{\partial T}{\partial x_j}\right) \tag{12}$$

The characteristic velocities are given as the solution of the eigenvalue problem and are $\lambda_1 = u - c_{norm}$, $\lambda_2 = \lambda_3 = \lambda_4 = u$ and $\lambda_5 = u + c_{norm}$, where c_{norm} is a normalized speed of sound, $c^2_{norm} = \frac{1}{\gamma M^2}\frac{\gamma p}{\rho}$. A normalized pressure is $p_{norm} = \frac{1}{\gamma M^2} p$. λ_1 and λ_5 are the velocities of sound waves moving in the negative and positive x-directions, λ_2 is the convection velocity (the speed of entropy waves) while λ_3 and λ_4 are the velocities at which v and w are advected in the x-direction. The system of Eqs. (8)-(12) includes derivatives normal to the $x = 0$ or L_x-boundary (d_1 to d_5),

$$d = \begin{pmatrix} \frac{1}{c^2_{norm}}\left[L_2 + \frac{1}{2}(L_5 + L_1)\right] \\ \frac{1}{2}(L_5 + L_1) \\ \frac{1}{2\rho c_{norm}}(L_5 - L_1) \\ L_3 \\ L_4 \end{pmatrix} = \begin{pmatrix} \frac{\partial(\rho u)}{\partial x} \\ \frac{\partial}{\partial x}(c^2_{norm}\rho u) + (1-\gamma) u \frac{\partial p_{norm}}{\partial x} \\ u\frac{\partial u}{\partial x} + \frac{1}{\rho}\frac{\partial p_{norm}}{\partial x} \\ u\frac{\partial v}{\partial x} \\ u\frac{\partial w}{\partial x} \end{pmatrix} \tag{13}$$

where the L_i's are the amplitudes of characteristic waves associated with each characteristic velocity λ_i. The L_i's are given by :

$$L_1 = \lambda_1\left(\frac{\partial p_{norm}}{\partial x} - \rho c_{norm}\frac{\partial u}{\partial x}\right) \tag{14}$$

$$L_2 = \lambda_2\left(c^2_{norm}\frac{\partial \rho}{\partial x} - \frac{\partial p_{norm}}{\partial x}\right) \quad L_3 = \lambda_3\frac{\partial v}{\partial x} \quad L_4 = \lambda_4\frac{\partial w}{\partial x} \quad L_5 = \lambda_5\left(\frac{\partial p_{norm}}{\partial x} + \rho c_{norm}\frac{\partial u}{\partial x}\right) \tag{15}$$

2.1 Subsonic inflow

At the inlet, it was chosen to impose the velocities, u, v and w, as well as the temperature, T, using the solution of the fully-developed channel flow, domain 1. The only remaining unknown is the density ρ which can be obtained through the continuity equation. For a subsonic three-dimensional flow, the only characteristic variable L_1 propagates against the flow direction, while the other four, L_2, L_3, L_4 and L_5, are entering the domain. L_1 is computed from the interior of the spatially developing channel using Eq. (14). The entering characteristic variables L_5 and L_2 are estimated,

$$L_5 = L_1 - 2\rho c_{norm}\frac{\partial u}{\partial t} \tag{16}$$

$$L_2 = \frac{1}{2}(\gamma - 1)(L_5 + L_1) + \frac{\rho c^2_{norm}}{T}\frac{\partial T}{\partial t} \tag{17}$$

Density is avanced in time using Eq. (8) and thus, it is strongly coupled to both velocity and temperature fluctuations in the periodical channel domain 1.

2.2 Turbulent realistic inflow

Equations (16) and (17) are fed with the velocity and temperature turbulent fields computed in domain 1. Domain 1 consists of a fully developed turbulent channel flow. For the incompressible case, the strategy to drive the flow at constant mass flux consists of adding, on the right hand side (*rhs*) of the momentum equation, a source term f [19] which can be viewed as a mean favourable pressure gradient. For the compressible case, and by analogy with this procedure the present strategy to transfer energy to the flow at constant total energy consists of adding, on the *rhs* of the total energy equation, a source term $\mathcal{W}$ which can be viewed as the rate of work produced by a mean streamwise enthalpy flux [8].
For compressible channel flow, it is customary to consider the source term f in the momentum equation as an external force to the flow system [1, 6, 2, 3, 4, 7, 5]. In the present study we do not consider such assumption,

but derive a source term by seeking a homogeneous velocity and density solution for the full compressible Navier-Stokes equations. Pressure and thus internal energy and the temperature are split into homogeneous and non-homogeneous contributions, while density is considered as homogeneous in the streamwise direction, which is consistent with both the continuity equation and the ideal gas law,

$$p = \bar{P}_o(x) + \bar{p}(x,y,z,t) \tag{18}$$
$$\rho\epsilon = (\bar{\rho}\tilde{\epsilon})_o(x) + \bar{\rho}\tilde{\epsilon}(x,y,z,t) \tag{19}$$
$$\rho T = (\bar{\rho}\tilde{T})_o(x) + \bar{\rho}\tilde{T}(x,y,z,t) \tag{20}$$

Consequently, the corresponding source term is not equivalent to the work of an external force and $\bar{\rho}\tilde{T}$ can be homogeneous. In the present formulation the pressure drop affects directly the streamwise evolution of the thermodynamic pressure [8]. A significant mean internal energy loss is induced $\frac{d(\bar{\rho}\tilde{\epsilon})_o}{dx} = \frac{1}{\gamma-1}\frac{d\bar{P}_0}{dx}$, and thus a negative streamwise temperature gradient appears and is compensated by wall heat flux. Since density is assumed to be homogeneous, the mean temperature gradient can be expressed at the wall by $\frac{dT_w}{dx} = \frac{1}{\rho_w}\frac{d\bar{P}_0}{dx}$, and $\frac{\tilde{T}-T_w}{T_w} = \frac{\rho_w-\overline{\rho}}{\bar{\rho}}$ is homogeneous.

2.3 Subsonic outflow

For non-reflecting subsonic outflow, L_2, L_3, L_4 and L_5 are computed using Eqs. (15) and the incoming wave L_1 has to be modeled. Poinsot & Lele [9] suggest to set

$$L_1 = L_1^{wave} + L_1^{exact} \tag{21}$$

Following Rudy & Strikwerda [20], [21] we model $L_1^{wave} = (1-M_l)c_{norm}\frac{p-p_{\inf}}{L}$, where M_l is the local Mach number. The exact par for L_1 is estimated in the present work, based on the pressure drop model, $L_1^{exact} = -(1-M_l)c_{norm}\, f$.
For the Navier-Stokes equations, some more viscous conditions have to be added [9] to be consistent with the *rhs* of equations (10-14). A basic model consists of setting this contributions to zero (present results). In the final contribution, results will describe the effect of such terms in the present flow configuration involving non-zero streamwise temperature gradients. A simple model is derived from the source involved in domain 1,

$$\frac{\partial(\mu S_{1j})}{\partial x_j} = \frac{\partial(\mu S_{3j})}{\partial x_j} \simeq 0 \tag{22}$$
$$\frac{\partial(\mu S_{2j})}{\partial x_j} \simeq \frac{\partial\mu}{\partial x}\frac{\partial u}{\partial y} \simeq 0.7\frac{\gamma M^2 Re}{\rho_w T_w} f^2 \tag{23}$$
$$\frac{\partial}{\partial x_j}\left(\mu\frac{\partial T}{\partial x_j}\right) \simeq \frac{\partial\mu}{\partial x}\frac{\partial T}{\partial x} \simeq \gamma^2 M^4 \frac{0.7\mu_w}{\rho_w^2 T_w} f^2 \tag{24}$$

3 Numerical results

Statistics performed on LES data are computed in time and space in the spanwise z direction (the only one homogeneous direction in the present case). Figure 2 shows the streamwise x-distribution for the velocity, temperature and pressure along the channel on the centerline and at the first grid point near the wall. Numerical results show that mean velocity is constant along the channel while both mean temperature and mean pressure decrease linearly with x. The slope of the mean pressure distribution is close to the pressure drop equivalent to the source f model derived in domain 1 (symbols). The scatter with the model at the outflow boundary will be discussed in the final contribution. An important aspect of the flow is the linear streamwise decrease of the mean temperature which confirms the validity of the model derived for domain 1. Mean density (not shown) is constant along x, which is consistent with asumptions performed for the inflow conditions. Figure 3 shows isovalues in the $x-y$ slice for the mean velocity, mean temperature and mean pressure. The results obtained on the centerline of the channel are confirmed for the whole channel. Velocity is roughly constant along x, pressure is independent of y and temperature is a function of both x and y, which is consistent with analytical solutions derived for such flow [8]. We note a slight defelection of the pressure isovalue in the near-wall region. The effect of outflow boundary conditions on such behaviour will be discussed in the final contribution.
Figure (4) is a comparison between the domain 1 (left) and the domains 2-7 (right) for the mean velocity profiles in the channel wall-normal direction. The same behaviour is obtained and nearly no transient exists in the spatially developing case, which means that inflow boundary conditions are correct. We note that spanwise and transverse velocities are not exactly zero, which could be related to a compressibility effect and has to be linked with the slight deflection of the pressure isovalues in the wall normal direction. Figure (5) is a similar comparison for temperature, pressure and density. The temperature is normalised by the wall temperature

which is linearly decreasing and therefore the profile of reduced temperature is independent of the streamwise postition along the channel. Mean pressure is uniformly decreasing from one domain to the next due to the constant pressure drop. Finally mean density is uniform along x and is increasing at the wall since pressure is constant along y.

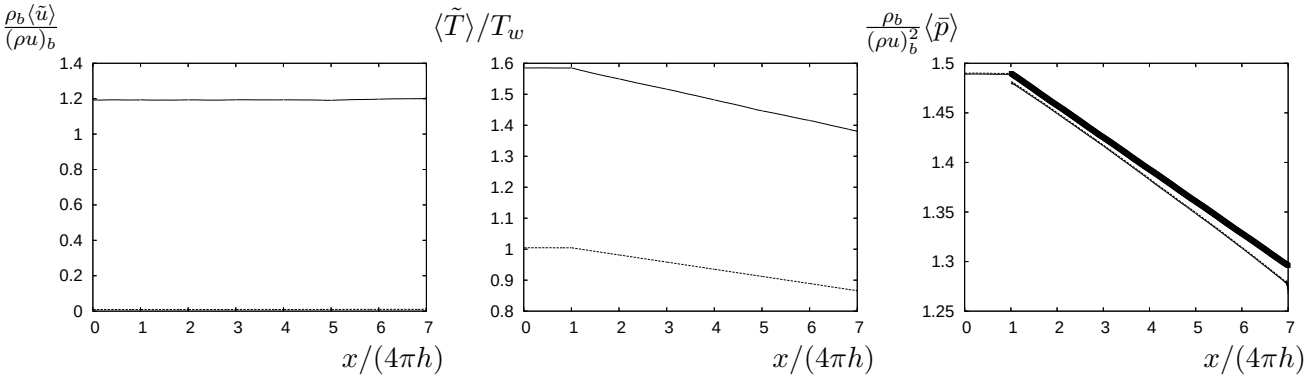

FIG. 2 – Mean streamwise velocity (a), temperature (b) and pressure (c). Streamwise distribution on the centerline (——) and at the first grid point in the wall-normal direction (- - -).

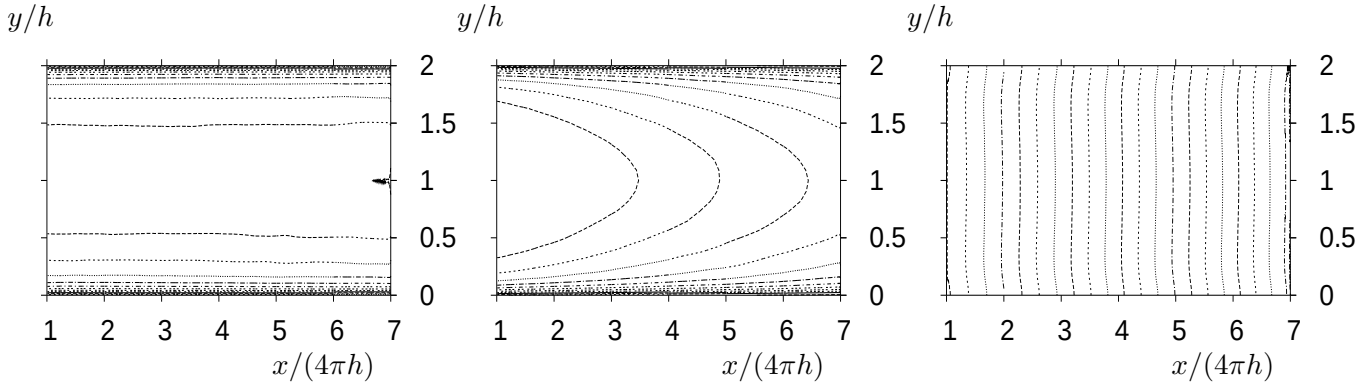

FIG. 3 – Isovalues of mean streamwise velocity (a), mean temperature (b) and mean pressure (c)

4 Conclusion

LES of spatially developping compressible channel flow were performed for $Re = 4,880$ and $M = 0.7$. The present results show that the main trends for spatially developing compressible channel flow are a constant pressure drop and a constant temperature loss in the streamwise direction. The assumption that density is conserved is verified in practice based on LES computations for a channel with a length of about $88\ h$. Further results involving outflow boundary conditions effects, compressibility effects and distorsion effects by mean of adverse pressure gradient will be discussed in the final contribution.

Références

[1] Coleman G., Kim J., and Moser R. A numerical study of turbulent supersonic isothermal-wall channel flow. J. Fluid Mech., 305, 159–183, 1995.

[2] Lechner R., Sesterhenn J., and Friedrich R. Turbulent supersonic channel flow. Journal of Turbulence, 2, 01–25, 2001.

[3] Lenormand E. and Sagaut P. Subgrid-scale models for large-eddy simultions of compressible wall bounded flows. AIAA J., 38, 1340–1350, 2000.

[4] Lenormand E., Sagaut P., and Ta Phuoc L. Large-eddy simulation of subsonic and supersonic channel flow at moderate reynolds number. Int. J. Num. Meth. Fluids, 32, 369–406, 2000.

[5] Salinas Vásquez M. and Métais O. Large-eddy simulation of the turbulent flow through a heated square duct. J. Fluid Mech., 453, 201–238, 2002.

[6] Foysi H., Sarkar S., and Friedrich R. Compressibility effects and turbulence scalings in supersonic channel flow. J. Fluid Mech., 509, 207–216, 2004.

[7] Morinishi Y., Tamano S., and Nakabayashi K. Direct numerical simulation of compressible turbulent channel flow between adiabatic and isothermal walls. J. Fluid Mech., 502, 273–308, 2004.

[8] Brun C., Petrovan Boiarciuc M., Haberkorn M., and Comte P. Large eddy simulation of compressible channel flow. arguments in favour of universality of compressible turbulent wall bounded flows. Theor. Comput. Fluid Dyn., 21, 2008.

[9] Poinsot T. and Lele S. Boundary conditions for direct simulations of compressible viscous flows. J. Comp. Phys., 103, 16–42, 1992.

[10] Comte P. and Lesieur M. Large-eddy simulations of compressible turbulent flows. In Advances in turbulence modelling, pages 77–79. Von Karman Institute, 1998. lecture series 1998-05.

[11] Métais O. and Lesieur M. Spectral large-eddy simulation of isotropic and stably stratified turbulence. J. Fluid Mech., 239, 157–194, 1992.

[12] Lesieur M. and Métais O. New trends in large-eddy simulations of turbulence. Annu. Rev. Fluid. Mech., 28, 45–82, 1996.

[13] Ducros F., Comte P., and Lesieur M. Large-eddy simulation of transition to turbulence in a boundary layer developing spatially over a flat plate. J. Fluid Mech., 326, 1–36, 1996.

[14] Gottlieb D. and Turkel E. Dissipative two-four methods for time-dependent problems. Math. Comp., 30, 703–723, 1976.

[15] Kennedy C. and Carpenter M. Comparison of several numerical methods for simulation of compressible shear layers. NASA technical paper, 3484, 1997.

[16] Kovasznay L. Turbulence in supersonic flow. J. Aeronautical Sciences, 20(10), 657–682, 1953.

[17] Thompson K. W. Time dependent boundary conditions for hyperbolic systems. J. Comp. Phys., 68, 1–24, 1987.

[18] Thompson K. Time-dependent boundary conditions for hyperbolic systems ii. J. Comp. Phys., 89, 439–461, 1990.

[19] Kim J., Moin P., and Moser R. Turbulence statistics in fully-developed channel flow at low reynolds number. J. Fluid Mech., 177, 133–166, 1987.

[20] Rudy D. and Strikwerda J. A nonreflecting outflow boundary condition for subsonic navier-stokes calculations. J. Comp. Phys., 55(70), 36, 1980.

[21] Rudy D. and Strikwerda J. Boundary conditions for subsonic compressible navier-stokes calculations. Computers and Fluids, 9, 327–338, 1981.

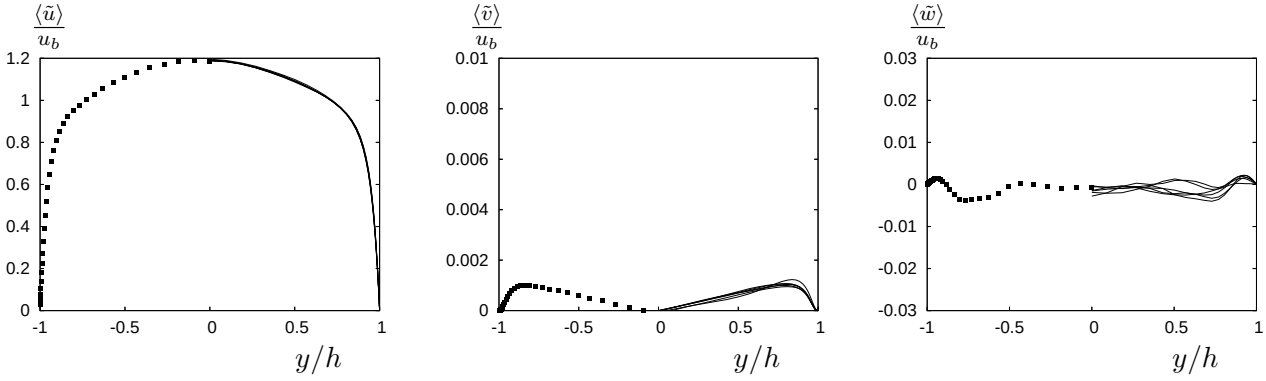

FIG. 4 – Profiles of (a) mean streamwise velocity, (b) mean wall-normal velocity, (c) spanwise velocity. Fully developed channel domain 1 (■) and spatial computational boxes domains 2-7 (——).

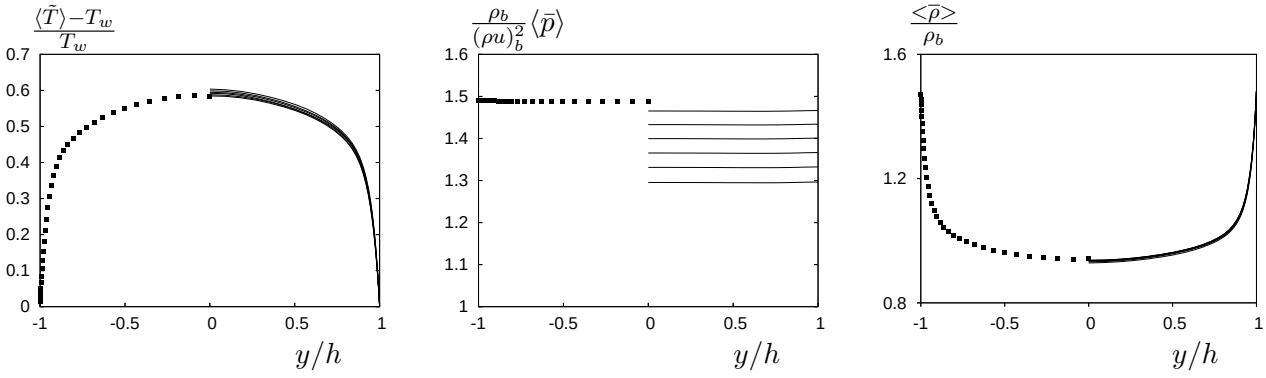

FIG. 5 – Profiles of (a) mean temperature, (a) mean pressure, (c) mean density. Fully developed channel domain 1 (■) and spatial computational boxes domains 2-7 (——).